Title: Multistage Microfluidic Platform for the Continuous Synthesis of III-V Core/Shell Quantum Dots

Authors: Jinyoung Baek; Yi Shen; Ioannis Lignos; Moungi G. Bawendi; Klavs F. Jensen, Ph.D.

To be cited as: 10.1002/anie.201805264

Link to VoR: https://doi.org/10.1002/anie.201805264

Multistage Microfluidic Platform for the Continuous Synthesis of III-V Core/Shell Quantum Dots

Jinyoung Baek[a,b,‡], Yi Shen[a,‡], Ioannis Lignos [a,c], Moungi G. Bawendi[c], and Klavs F. Jensen*[,a]

Abstract: We present a fully continuous chip microreactor based multistage platform for the synthesis of heterostructural quantum dots. The use of custom-designed chip reactors enables precise control of heating profiles and flow distribution across the microfluidic channels while conducting multistep reactions. The platform can be easily reconfigured by reconnecting the differently designed chip reactors allowing for screening of various reaction parameters during the synthesis of nanocrystals. III-V based core/shell structures are chosen as model reaction systems, including InP/ZnS, InP/ZnSe, InP/CdS and InAs/InP, which are prepared in flow using a maximum of 6 chip reactors in series.

Quantum dots (QDs) have attracted significant attention due to their size-tunable photophysical properties[1]. The most studied QD systems are Cd-based and Pb-based materials, which are restricted in highly regulated applications[2]. Among the Cd- and Pb-free semiconductor nanocrystals, III-V QDs stand out as the most promising alternatives for optoelectronic applications[2–4]. The synthesis of III-V QDs often undergoes more than one step as clusters are initially formed as critical intermediates[5–8]. Therefore, multi-step synthesis is commonly employed to prepare III-V QDs in a sequential manner[9,10]. Additionally, to improve the stability and brightness of III-V QDs, higher band gap materials, such as ZnS and CdS, are often used, which can passivate the surface sites of III-V QDs[11,12]. As a result, to transfer this multistep synthesis of III-V core/shell QDs to continuous nanomanufacturing, we need to develop multistage high-temperature reactors with consecutive reaction steps.

Over the past decade, microfluidic technology has been widely applied to nanocrystal synthesis and reaction optimization[13,14], characterization of reaction kinetics[15,16], purification[17] and surface modification[18]. Compared to traditional batch-based processes, flow-based configurations can improve mass and heat transfer and precisely control reaction parameters, which is ideal for large-scale nanomanufacturing[13,19]. Despite extensive research on the synthesis of nanocrystals with a homogeneous structure, few studies have focused on the preparation of nanocrystals with heterostructures (like core/shell morphologies) in flow[20,21]. One possible reason is that the synthesis of heterogeneous structures often requires slow additions of the overcoating precursors to avoid secondary nucleation of the shell material, which is challenging to achieve using tubular reactors or droplet-based systems[20,21].

In this work, we have implemented multistage high-temperature and high-pressure silicon-pyrex chip reactors (up to 6 stages) to synthesize various III-V based core/shell QDs in flow. The customized chip reactors with different heating profiles and flow distributions are assembled with ease to precisely control the reaction conditions over different syntheses. The design of sub-channels in the shell-growth microreactors also allows us to maintain a low concentration of the shell precursors, which suppresses undesirable secondary nucleation. Utilizing this platform, we successfully prepared a series of InP/ZnS, InP/ZnSe, InP/CdS and InAs/InP QDs with narrow distributions at different wavelengths and high photoluminescence (PL) quantum yields (QYs).

A detailed description regarding the reactor design and the experimental procedure is available in the supporting information. The first model system that we investigated was the synthesis of InP/ZnS core/shell QDs. As shown in Figure 1a, six high-temperature and high-pressure micro-chip reactors were cascaded into a synthetic platform. Six consecutive reactions were intensified including mixing, aging, sequential growth, two shell formations, and one annealing process. The first three stages were similar to that reported in our previous study for the synthesis of high-quality InP cores (Figure S2)[10,22]. In a typical synthesis, for the first mixing stage we introduced a temperature gradient between 120 °C and 280 °C using a heating block, whereas the temperature of the aging and sequential growth stages was fixed to 320 °C. The high operating pressure (65 bar) allows us to utilize octane as the solvent, which provides excellent mixing and low dispersion for both core and core-shell growth at or near supercritical conditions[23,24].

[a] Dr. J Baek, Dr. Y Shen, Dr. I Lignos and Prof. KF Jensen
Department of Chemical Engineering
[c] Dr. I Lignos and Prof. MG Bawendi
Department of Chemistry
Massachusetts Institute of Technology
77 Massachusetts Ave, Cambridge, MA 02139, United States
E-mail: kfjensen@mit.edu
[b] The Boston Consulting Group, Seoul 04539, Korea
[‡] JB and YS contributed equally.
Supporting information for this article is given via a link at the end of the document.
Massachusetts Institute of Technology, Massachusetts, 02139, United

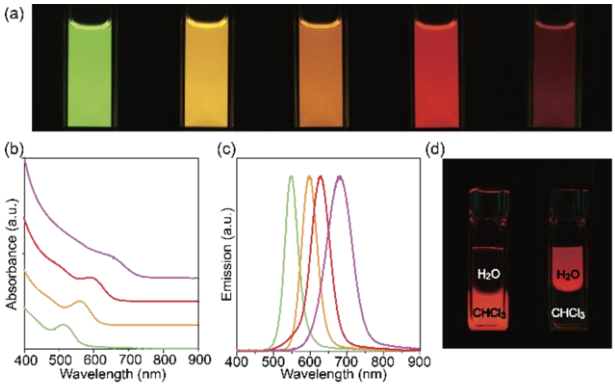

Figure 2. (a) A photograph of InP/ZnS QDs of various sizes illuminated under 365 nm UV light. Their PL peaks located at 554, 599, 605, 630, and 681 nm (from left to right). (b, c) Absorption and emission spectra of the InP/ZnS QDs depicted in Figure 2a. (The spectra of the QDs emitting at 605 nm are not included) (d) Phase transfer of InP/ZnS QDs from chloroform (left) to water (right) after ligand exchange with 3-mercaptopropionic acid. The mixtures were also illuminated under 365 nm UV light.

growth reactors) are used for the synthesis of InP cores and the following three-stages (two shell formation reactors and one annealing reactor) for the synthesis core/shell morphologies. (b) The design of the shell-formation microreactor consisting of ten sub-channels.

Monodisperse InP cores, that have a diameter of 2 nm and their first absorption peak between 510 and 520 nm, were synthesized after the first two reaction stages. By alternating injections of additional molecular precursors into the third microreactor, we managed to obtain InP QDs exhibiting band-edge absorption up to 595 nm with precise control. Preparation of larger InP cores (band-edge absorption higher than 600 nm) remains a synthetic challenge [9,11]. In this work, we introduced extra myristic acid to overcome the growth limitation, which simultaneously promotes the ripening of nanoparticles and broadens particle size distribution.

For the formation of InP/ZnS core/shell morphologies, the InP cores with various controlled diameters were continuously flowed into the shell formation microreactors without incorporating any additional purification process. $Zn(OA)_2$ and $(TMS)_2S$ were first used as the precursors for ZnS shell formation. To prevent undesired ZnS nucleation, we designed a microreactor having ten sub-channels maintaining a low concentration of the shell materials during the overcoating process (Figure 1b and Figure S3). Importantly, to avoid any undesired back-flow, both the width and the depth of the sub-channels were designed to be 4~5 times smaller than that of main channel (see SI for detailed discussion). In a typical synthesis, each precursor solution was divided into five sub-channels before being injected into the main stream (each channel distributed 20±2% of the flow based on calculations). The temperature of the shell-formation microreactors was 250 °C, and the residence times were altered between 6 and 8

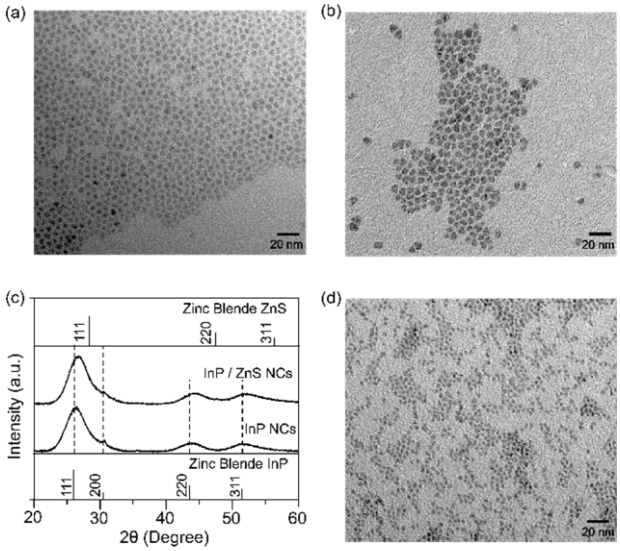

Figure 3 (a,b) TEM images of InP/ZnS core/shell QDs prepared with $Zn(OA)_2$ and $(TMS)_2S$ serving as shell precursors. The corresponding emission peaks of these samples were located at 630 nm (a) and 681 nm (b). (c) XRD patterns of InP core and InP/ZnS core/shell QDs. (d) InP/ZnS core-shell QDs synthesized using thiol instead of $(TMS)_2S$ as the sulfur precursor. The emission peak of this sample was 558 nm.

minutes depending on the flow-rate of the solution containing the InP cores. Two shell-formation microreactors were typically used during the growth providing better control of residence time. The platform was also equipped with one extra reactor for annealing (the annealing temperature was normally the same as the shell growth temperature) after shell formation. The system was monitored by a customized optical device to characterize the absorption and emission of QDs in-line.

By varying the size of InP cores, we successfully obtained InP/ZnS QDs with emission color ranging from green to red. Figure 2a is a color photograph showing the spectral range of InP/ZnS QD solutions under 365 nm UV excitation. Figure 2b-c show the absorption and emission spectra of those four InP/ZnS core/shell QDs. The PL peaks of those samples are located at 554 nm, 599 nm, 630 nm, and 681 nm. The full-width-at-half-maximum (FWHM) of those peaks were as low as 42 nm for those emitting at 554 nm. These narrow emissions could be attributed to the advantages of enhanced mixing in supercritical octane. The PL QYs of the InP/ZnS core/shell QDs were as high as 40% for the 554 nm emitting QDs and 32% for the 630 nm emitting QDs after one cycle of precipitation/redissolution. In addition, the as-synthesized InP/ZnS QD samples can be transferred into phosphate buffered saline (PBS) after the ligand exchange reaction with 3-mercaptopropionic acid. As shown in Figure 2d, the exchanged sample remains luminescent in aqueous media, which indicates that the ZnS shell uniformly overcoates the InP cores.

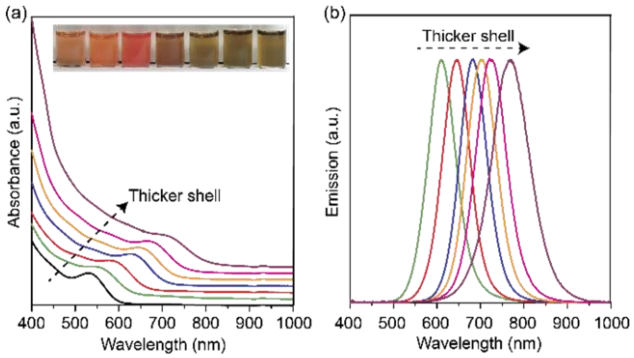

Figure 4. Absorption (a) and emission (b) spectra of the InP/CdS QDs with the same core sizes and different shell thicknesses. The black line in (a) is the absorption spectrum of the InP cores. The inset in (a) is a picture of all the samples in ambient light.

Table 1 A list of the synthesized III-V core/shell QDs using the multistage platform.

Core/shell QDs	Reaction Platform	Emission range (nm)	Highest QY	Average FWHM (meV)
InP/ZnS	6-stage: Mixing; Aging; Sequential growth; Shell formation ×2; Annealing	554 – 681	40%	187±24
InP/ZnSe	5-stage: Mixing; Aging; Sequential growth; Shell formation; Annealing	582 – 647	45%	195±4
InP/CdS	4-stage: Mixing; Aging; Shell formation; Annealing	608 – 768	50%	215±20
InAs/InP	3-stage: Mixing; Aging; Shell formation	680 – 783	35%	170±7

The sizes of the InP/ZnS core/shell QDs were further characterized by transmission electron microscopy (TEM) (Figure 3a-b). The average sizes of InP/ZnS core/shell QDs measured from the images are 4.1 and 4.9 nm. The band-edge absorption peaks of these two samples are located at 590 nm and 657 nm. Based on the sizing curve of pure InP QDs, we estimate the sizes of the particles to be 3.4 nm and 4.3 nm, which are smaller than the measured values from TEM. This result is consistent with the formation of a shell on the InP core surface. X-ray diffraction (XRD) patterns of InP cores suggest a zinc blende structure (Figure 3c). The small shift of the peaks between InP QDs and InP/ZnS core/shell QDs indexed to the (111), (220), and (311) planes is likely due to the strain at the interface between InP core and ZnS shell[25,26]. The composition of these samples was also characterized by wavelength dispersive spectroscopy (WDS) after multiple precipitation/redissolution cycles, which further proves the successful formation of ZnS shell on InP core (Table S1).

Short-chain alkyl thiols, such as 1-dodecanethiol and 1-hexanethiol can also be used for the synthesis of the ZnS shell[27]. Using that synthetic route, InP/ZnS core/shell QDs emitting at 558 nm with an average diameter of 3.8 nm were synthesized (Figure 3d). The PL QY was as high as 35%. Although 1-hexanethiol has a low boiling point (150-160 °C) at ambient conditions, it can still be used in our pressure-tolerant platform. This result is a demonstration of the use of precursors that are not suitable for conventional batch synthesis. In addition, we have successfully coated ZnSe shells on InP cores. Compared to ZnS, it is easier to form a thicker ZnSe shell on the InP surface due to a smaller lattice mismatch[28]. The emission peaks of the samples were tunable from 582 nm to 647 nm with QY values ranging from 35% to 45% (Figure S4). However, the stability of InP/ZnSe QDs was limited, and the fluorescence was completely quenched after the ligand exchange reaction with 3-mercaptopropionic acid.

To gain full control of the reaction process, we evaluated the capability of tuning the shell thickness using our platform. Among all the commonly used shell materials for InP cores, CdS has the smallest lattice mismatch (Table S2), which makes it more feasible to control the shell thickness on the core surface. For this reason, we decided to synthesize a series of InP/CdS QDs, using our four-stage reaction platform: mixing, aging, shell growth and annealing. The shell formation temperature was maintained between 290 °C and 300 °C, whereas that of the annealing reactor was maintained between 280 °C and 330 °C. By varying the flow rates of the shell precursors, we successfully obtained InP/CdS QDs with different shell thicknesses using the same InP cores. Detailed experimental conditions are summarized in Table S3. As shown in Figure 4, when more shell precursors were dosed, thicker shells were formed on the InP cores as indicated by the red-shift of the corresponding absorption and PL peaks. The particles were still roughly spherical as illustrated in the representative TEM images (Figure S5). The synthesized InP/CdS samples exhibited high brightness and relatively narrow distribution (Table S3). For example, the QY of the particles emitting at 608 nm was 50% with 75 nm in FWHM.

Other than InP core based QDs, we also prepared a series of hetero-structural QDs using InAs as the core material. For example, InAs/InP QDs were prepared using a 3-stage reactor platform. InAs cores were synthesized in the first two stages (mixing and aging), and the overcoating process was accomplished by one shell-formation microreactor. The temperatures of each reactor were fixed at 120 °C, 290 °C and 230 °C, respectively. When higher concentrations of InP shell materials were dosed into the platform, both absorption and PL peaks red-shifted. By varying the flow rates of the InP shell precursors, we were able to tune the emission maxima of the samples from 680 nm to 783 nm (Figure S6), while the QY of the synthesized QDs was 30%- 35%, which is reasonable for the pure III-V QDs.[29] Similar to previous studies in the literature, the fluorescence of InAs/InP QDs was maintained after exposure to air[29]. This result also suggests that a complete InP shell was overcoated on the core surface, which protects InAs from oxidation[29].

In summary, we presented a multistage high-temperature and high-pressure chip reactor platform to synthesize various III-V based core/shell nanostructures in a continuous manner (Table 1). The custom design of a novel silicon-pyrex chip reactor with sub-channels allows for the slow addition of shell precursors into the core stream, which suppresses secondary nucleation of shell particles. The differently designed silicon-chip reactors can be connected with ease to allow for the synthesis of nanocrystals in various temperatures and injection profiles.

Importantly, the intensified consecutive synthetic platform significantly shortens the total processing time. For example, the residence time for the synthesis of InP/CdS core/shell QDs emitting at 768 nm was less than 4.5 minutes. This designed platform allows the formation of III-V based QDs of comparable quality with those obtained from batch methods. To further improve the quality of the synthesized nanocrystals, better control over the III-V QD growth process is necessary, in which case, this platform can also serve as an ideal tool for reaction parameter screening. Addition of another unit operation, such as purification, into the platform will accelerate the continuous nanomanufacturing of complex structures.

Acknowledgements

This work is supported by the National Science Foundation under grant no. ECCS-1449291 and CHE-0714189. J. Baek was supported by a Samsung Scholarship from the Samsung Foundation of Culture. I. Lignos was supported by a Swiss National Foundation Grant P2EZP2_172127. We thank Dr. Peter Allen, Dr. Daniel Harris and Dr. Samuel Marre for helpful discussion.

Keywords: Core/shell, Flow synthesis, Microfluidic reactor, Multistage, III-V QDs

References

[1] J. Owen, L. Brus, *J. Am. Chem. Soc.* **2017**, *139*, 10939–10943.
[2] S. Tamang, C. Lincheneau, Y. Hermans, S. Jeong, P. Reiss, *Chem. Mater.* **2016**, *28*, 2491–2506.
[3] P. Reiss, M. Carrière, C. Lincheneau, L. Vaure, S. Tamang, *Chem. Rev.* **2016**, *116*, 10731–10819.
[4] G. Xu, S. Zeng, B. Zhang, M. T. Swihart, K.-T. Yong, P. N. Prasad, *Chem. Rev.* **2016**, *116*, 12234–12327.
[5] B. M. Cossairt, *Chem. Mater.* **2016**, *28*, 7181–7189.
[6] D. C. Gary, M. W. Terban, S. J. L. Billinge, B. M. Cossairt, *Chem. Mater.* **2015**, *27*, 1432–1441.
[7] D. C. Gary, S. E. Flowers, W. Kaminsky, A. Petrone, X. Li, B. M. Cossairt, *J. Am. Chem. Soc.* **2016**, *138*, 1510–1513.
[8] L. Xie, Y. Shen, D. Franke, V. Sebastián, M. G. Bawendi, K. F. Jensen, *J. Am. Chem. Soc.* **2016**, *138*, 13469–13472.
[9] D. Franke, D. K. Harris, O. Chen, O. T. Bruns, J. A. Carr, M. W. B. Wilson, M. G. Bawendi, *Nat. Commun.* **2016**, *7*, 12749.
[10] Baek Jinyoung, Allen Peter M., Bawendi Moungi G., Jensen Klavs F., *Angew. Chem. Int. Ed.* **2010**, *50*, 627–630.
[11] E. Bang, Y. Choi, J. Cho, Y.-H. Suh, H. W. Ban, J. S. Son, J. Park, *Chem. Mater.* **2017**, *29*, 4236–4243.
[12] Reiss Peter, Protière Myriam, Li Liang, *Small* **2009**, *5*, 154–168.
[13] I. Lignos, R. Maceiczyk, A. J. deMello, *Acc. Chem. Res.* **2017**, *50*, 1248–1257.
[14] L.-J. Pan, J.-W. Tu, H.-T. Ma, Y.-J. Yang, Z.-Q. Tian, D.-W. Pang, Z.-L. Zhang, *Lab. Chip* **2017**, *18*, 41–56.
[15] I. Lignos, S. Stavrakis, G. Nedelcu, L. Protesescu, A. J. deMello, M. V. Kovalenko, *Nano Lett.* **2016**, *16*, 1869–1877.
[16] M. Abolhasani, C. W. Coley, L. Xie, O. Chen, M. G. Bawendi, K. F. Jensen, *Chem. Mater.* **2015**, *27*, 6131–6138.
[17] Y. Shen, N. Weeranoppanant, L. Xie, Y. Chen, M. R. Lusardi, J. Imbrogno, M. G. Bawendi, K. F. Jensen, *Nanoscale* **2017**, *9*, 7703–7707.
[18] Shen Yi, Abolhasani Milad, Chen Yue, Xie Lisi, Yang Lu, Coley Connor W., Bawendi Moungi G., Jensen Klavs F., *Angew. Chem. Int. Ed.* **2017**, *56*, 16333–16337.
[19] Y. Pu, F. Cai, D. Wang, J.-X. Wang, J.-F. Chen, *Ind. Eng. Chem. Res.* **2018**, *57*, 1790–1802.
[20] M. S. Naughton, V. Kumar, Y. Bonita, K. Deshpande, P. J. A. Kenis, *Nanoscale* **2015**, *7*, 15895–15903.
[21] A. Yashina, I. Lignos, S. Stavrakis, J. Choo, A. J. deMello, *J. Mater. Chem. C* **2016**, *4*, 6401–6408.
[22] S. Marre, A. Adamo, S. Basak, C. Aymonier, K. F. Jensen, *Ind. Eng. Chem. Res.* **2010**, *49*, 11310–11320.
[23] Marre Samuel, Park Jongnam, Rempel Jane, Guan Juan, Bawendi Moungi G., Jensen Klavs F., *Adv. Mater.* **2008**, *20*, 4830–4834.
[24] A. Chakrabarty, S. Marre, R. F. Landis, V. M. Rotello, U. Maitra, A. D. Guerzo, C. Aymonier, *J. Mater. Chem. C* **2015**, *3*, 7561–7566.
[25] E. Ryu, S. Kim, E. Jang, S. Jun, H. Jang, B. Kim, S.-W. Kim, *Chem. Mater.* **2009**, *21*, 573–575.
[26] L. Li, P. Reiss, *J. Am. Chem. Soc.* **2008**, *130*, 11588–11589.
[27] O. Chen, J. Zhao, V. P. Chauhan, J. Cui, C. Wong, D. K. Harris, H. Wei, H.-S. Han, D. Fukumura, R. K. Jain, et al., *Nat. Mater.* **2013**, *12*, 445–451.
[28] K. R. Reid, J. R. McBride, N. J. Freymeyer, L. B. Thal, S. J. Rosenthal, *Nano Lett.* **2018**, *18*, 709–716.
[29] Cao Yun- Wei, Banin Uri, *Angew. Chem. Int. Ed.* **1999**, *38*, 3692–3694.

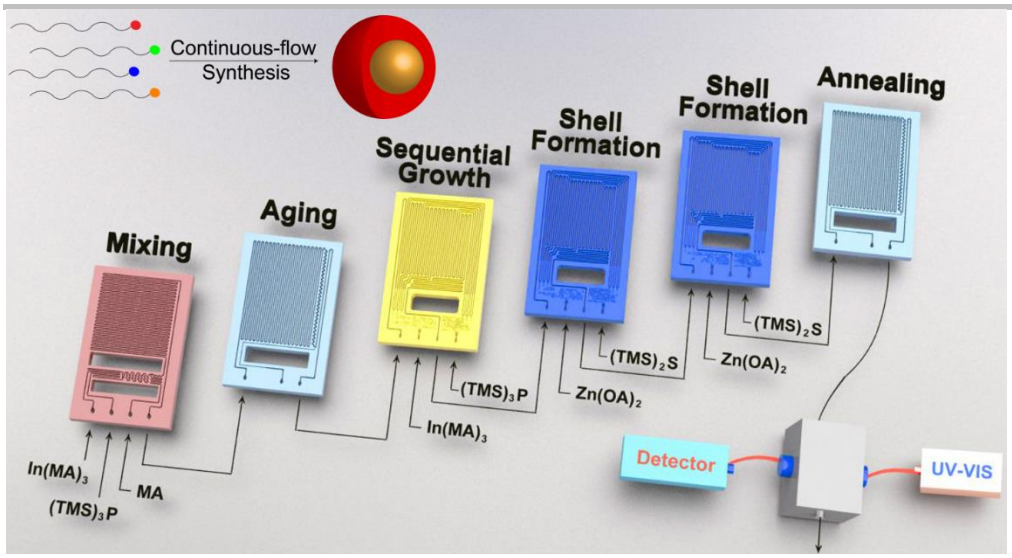

We present a multistage microfluidic platform to synthesize quantum dots with heterostructures in a continuous fashion. By cascading a variety of custom designed silicon/pyrex chip reactors, we precisely control the temperature and flow distribution during both core synthesis and the overcoating reaction. Utilizing up to six reaction stages, we manage to synthesize four types of III-V based core/shell quantum dots with control over their core size and shell thickness.